Results in Engineering 26 (2025) 105158

Contents lists available at ScienceDirect

Results in Engineering

journal homepage: www.sciencedirect.com/journal/results-in-engineering

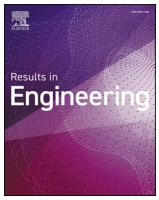

Research paper

Strength and stability of pultruded GFRP elements

Giuseppe Campione

Full Professor of Structural Engineering at Department of Engineering, University of Palermo, Viale delle Scienze, 90128 Palermo, Italy

ARTICLE INFO

Keywords:
Hollow circular cross-section
Ribs
Stiffeners
Critical stress
Critical load
Ultimate moment

ABSTRACT

The overall purpouse of this research was the proposal of a simple analytical expression for the calculus of critical stress and ultimate moment of a hollow cross-sections stiffened internally or externally with GFRP ribs. The model considers a compressed cylinder of small thickness composed of a set of meridians and parallels made of GFRP fiber beams connected and interacting with a containment action of the parallels on the meridians. The model also includes the cases of stiffened cross-section for the calculus of critical load for global buckling. Major findings were the determination of limits of diameter/thickness ratio of the profile suitable to avoid premature failures due to buckling before material crushing. Limits were 10 for a profile without stiffeners and between 18 and 25 for profiles with stiffeners. The global buckling load increases with the presence of internal stiffeners with increases of up to 100 % compared to the case of elements without stiffeners. In bending, it was found that the ovalization of the section significantly reduces the critical moment due to buckling effects and also ovalization increases the flexibility of elements with deflection increased up to 100 % with respect to elements without ovalization. The importance of this study is the proposal of analytical expressions for strength verification of FRP pultruded elements under flexure and axial forces taking into account of second order effects derived though a mechanical model clear also to practioner engineers.

1. Introduction

Glass fibre reinforced polymer (GFRP) are becoming widely used because they are light and resistant to corrosion and find various applications such as lighting poles, electrification, bridges, infrastructure etc (see Fig. 1). Lightness is an important advantage of GFRP structures that makes them suitable for transportation. Non-corrodibility makes them competitive with steel structural elements. Steel structures in marine environments are prone to corrosion, and factors such as seawater salinity are known to accelerate this process. Reinforced concrete marine structures are subjected to chloride attacks, which reduce the alkalinity of concrete and result in corrosion of the reinforcing steel. Consequently, the maintenance and rehabilitation costs for marine and coastal infrastructure is very high and could be a severe economic burden and the used of GFRP becomes competitive with steel.

However, the use of FRP as a base material for structural elements in marine infrastructure and bridge has been limited. At present there are few codes (e.g. CEN/TS 19,101:2022, ASCE/SEI 74) that provide details on their design at the ultimate and serviceability limit states. To clarify the role and importance of the above observations, in this paper the problem of local and global stability of stiffened circular cross-section FRP pultruded piles is examined considering different stiffeners technique to increase the local and global buckling strength of elements with hollow circular cross-sections. In this paper a simple model to calculate the critical strength of circular hollow cross-sections with different stiffeners techniques is proposed taking into account also of the influences of stiffeners on the overall buckling load of structural elements. All these aspects have been widely discussed in the literature [1–10], but there is still no uniformity in the prediction formulas in all the available reference documents, both normative and pre-normative. In this work, the problem of local and global buckling, including the effects of ovalization of elements with circular cross-section, is examined and simple equations for the verification at the ultimate and serviceability limit state are provided, validated on the basis of experimental data available in the literature. Long time effects are considered in the present model as suggested in the litature by reducing the modulus of elasticity.

2. Strength and stability of members with GFRP cross-section

In this section, some expressions available in the literature are given for the calculation of the critical stress due to local buckling of pultruded members with double-T, circular or polygonal cross-section. Then, a new method for the calculation of the critical stress for circular cross-

E-mail address: giuseppe.campione@unipa.it.

https://doi.org/10.1016/j.rineng.2025.105158
Received 4 March 2025; Received in revised form 22 April 2025; Accepted 29 April 2025
Available online 7 May 2025

sections with stiffeners is proposed.

2.1. Compressive strength of material

With reference to the material compressive strength, compression tests are generally performed on stub elements to determine the compressive strength and the longitudinal elastic modulus; however, in the absence of this information, for a preliminary design of the elements it is possible to use analytical expressions available in literature, such as that of Cardoso et al. [11] which allows to calculate the compressive strength of the material starting from the value of the elastic tangential modulus G with the expression:

$$\sigma_m = G\cdot(1+\chi_{cr}/a)^b \tag{1}$$

a,b, χ_{cr} are coefficients assumed in Cardoso et al. [11] 0.21, −0.69, 5.148 and substituting them in Eq. (1) it becomes:

$$\sigma_m = 0.107\cdot G \tag{2}$$

In this work, the longitudinal elastic modulus of GFRP has been related to its compressive strength with a linear relationship of the form:

$$E_1 = 100\cdot\sigma_m \ \text{(MPa)} \tag{3}$$

By adopting Eq. (3) it is possible to construct the diagram of Fig. 2, which provides the variation of the longitudinal and tangential elastic modulus (Eq. (2)) with the compressive strength.

In the same graph, some experimental data available in literature are reported. It can be seen that the correlation proposed by Cardoso et al. [11] gives an excellent interpolation of the experimental data, when 1/9 E_1 is assumed for the modulus G.

Eq. (3) is safe with respect to the available experimental data and has the advantage that allows one to find the value of the longitudinal elastic modulus starting from the compressive strength, which can be easily determined with a compression test on a stub element.

2.2. Local buckling of cross-sections

In this section, the cases of thin-walled circular and double-T cross-sections are examined (See Fig. 3) and the analytical expressions for the calculation of the critical stress are provided for them.

Timoscenko and Gere [12] provide the expression of the critical stress of a rectangular plate of depth b and thickness t in the form:

$$\sigma_{cr} = k_v\cdot\frac{\pi^2\cdot E}{12\cdot(1-\upsilon^2)}\cdot\left(\frac{t}{b}\right)^2 \tag{4}$$

ν being the Poisson coefficient and k_v a coefficient depending on the boundary conditions and assumed 4 for a plate on two supports. E is the modulus of elasticity.

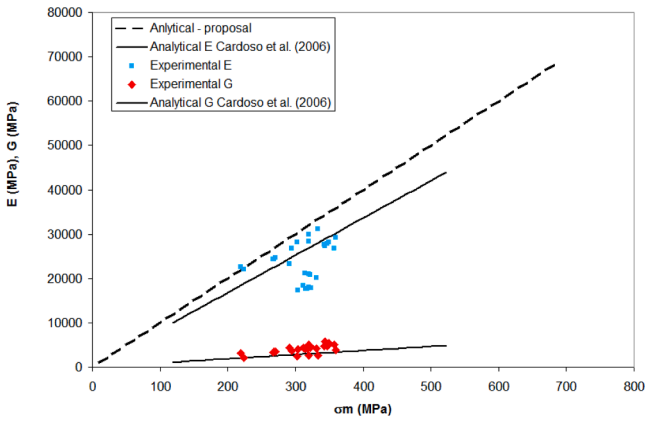

Fig. 2. Variation of longitudinal and shear modulus with compressive strength.

For a thin-walled circular cross-section of diameter D and thickness t loaded on the two bases by compressive forces it is well known from the literature [12] that the critical stress can be expressed as:

$$\sigma_{cr} = \frac{E}{\sqrt{3\cdot(1-\upsilon^2)}}\cdot\frac{2\cdot t}{D} \tag{5}$$

Cosenza and Pecce (2000) propose for double T-sections in GFRP an expression of the critical stress in the form:

$$\sigma_{cr} = k_r\cdot\frac{\pi^2\cdot E_1}{12\cdot(1-\nu_{12}{}^2)}\cdot\left(\frac{t}{b}\right)^2 \ \text{for}\ 0.3 \le \frac{b}{t_f}\cdot\frac{t_w}{h} \le 1.152 \tag{6}$$

$$k_r = \left(0.125+\frac{b}{t_f}\cdot\frac{t_w}{h}\right)\cdot\left(\frac{E_2}{E_1}\right)^{0.85} \tag{7}$$

b and h being the width and the eight of CFRP double T section, t_f and t_w the thickness of flange and web, E_1, E_2 the longitudinal and transversal module of elasticity and ν_{12} the Poisson coefficient.

Cardoso et al. [11] suggest for double-T sections to calculate the critical stress with the expression:

$$\sigma_{cr} = k_r\cdot\frac{\pi^2\cdot E_1}{12\cdot(1-\nu_{12}{}^2)}\cdot\left(\frac{t}{b}\right)^2 \tag{8}$$

being

$$k_r = \frac{2}{\sqrt{1+4/3\cdot\pi^2\cdot\eta^3}}\cdot\left(\frac{E_2}{E_1}\right)^{0.5} + \frac{2\cdot\nu_{12}\cdot E_2/E_1 + 4\cdot(1+\eta)\cdot(1-\nu_{12}{}^2)\cdot G/E_1}{\sqrt{1+4/3\cdot\pi^2\cdot\eta}} \tag{9}$$

With $\eta = b_f/b_w$.

Fig. 1. Structural application of GFRP elements for deck and bridge (photo of the author).

If we assume $G = 1/9E_1$, $\nu = 0.23$ Eq. (9) and Eq. (11) give 0.51 and 0.57 for E_1/E_2=1/3 and 0.83 and 0.73 for E_1/E_2=1/3 and 2/3 respectively. This results stressed that equations of Cardoso et al. (2006) give quite same results of that proposed by Cosenza and Pecce (2000).

The desing manual of Srongwell (2006) suggests for hollow section the empirical equation for critical stress in the form:

$$\sigma_{cr} = \frac{E_1}{16}\cdot\left(\frac{t}{D}\right)^{0.85} \tag{10}$$

For polygonal sections of side b, AASH (2009) suggest the expression:

$$\sigma_{cr} = 3.27\cdot\frac{E_1}{\left(1-\upsilon_{12}{}^2\cdot E_2/E_1\right)^{0.5}}\cdot\left(\frac{t}{b}\right)^2\cdot 0.5\cdot\left[\left(E_2/E_1\right)^{0.5}+\upsilon_{12}\cdot\left(E_2/E_1\right)+\left(2\cdot G\cdot\left(1-\upsilon_{12}{}^2\cdot E_2/E_1\right)/E_1\right)\right] \tag{11}$$

For hollow circular sections AASH (2009) suggests the expression:

$$\sigma_{cr} = 0.75\cdot\frac{E_1}{\left(1-\upsilon_{12}{}^2\cdot E_2/E_1\right)^{0.5}}\cdot\frac{t}{D}\cdot 1.414\cdot\left[\left(1+\upsilon_{12}\cdot\left(E_2/E_1\right)^{0.5}\right)\cdot\left(E_2/E_1\right)^{0.5}\cdot\left(G/E_1\right)\right]^{0.5} \tag{12}$$

It was here derived by the author an analytical expression to calculate the critical stress of the GFRP hollow circular section in the absence and presence of internal or external stiffeners such as those shown in Fig. 3.

In some cases, the stiffeners for GFRP cross-section consist of star-shaped or triangular-shaped ribs, all made of GFRP generally having of the same thickness of the hollow section. In other cases, cross-section are formed with non-corrugated or corrugated PVC hollow cross-section reinforced externally or internally (or only externally) with GFRP reinforcement layers.

The model for elements without stiffeners, considers a cylindrical shell of diameter D and thickness t loaded in compression. The cylinder has been idealized as a series of parallels that transversally connect the meridians (see Fig. 4). The generic meridian is considered as an elastic beam with a square cross-section of side t transversally constrained by GFRP ring beams with a square cross-section of side t. The meridian is therefore a beam on elastic springs.

Critical compression load can be obtained with the expression of Timoschenko and Gere [12] derived for an elastic beam on elastic soil and expressed as:

$$P_{cr} = 2\cdot\sqrt{E_1\cdot J\cdot k} \tag{13}$$

In the case in question, k, which is the stiffness of the springs, takes on the meaning of radial stiffness of a ring beam formed by the parallels and having the expression:

$$k = \frac{E_2\cdot t^2}{\left(1-\upsilon_{12}{}^2\right)\cdot\left(D/2\right)^2} \tag{14}$$

Substituting Eq. (16) into Eq. (15) it results:

$$P_{cr} = 2\cdot\sqrt{\frac{E_1\cdot t^4}{12\cdot\left(1-\upsilon_{12}{}^2\right)}\cdot\frac{E_2\cdot t^2}{\left(D/2\right)^2}} \tag{15}$$

the critical stress is derived from Eq.(15) divided by t^2 (area of meridian) resulting:

$$\sigma_{cr} = \frac{P_{cr}}{t^2} = 2\cdot\frac{t}{D}\cdot\sqrt{0.625\cdot\left(\frac{E_2}{E_1}\right)^{0.85}}\cdot\sqrt{\frac{E_1\cdot E_2}{3\cdot\left(1-\upsilon_{12}{}^2\right)}} \tag{16}$$

Since the GFRP material is orthotropic, as already done in Cosenza and Pecce (2000) for pultruded elements with a W-shaped cross-section, two correction coefficients were introduced in Eq. (16). The first one is 0.625 for hollow circular section and the second one is $(E_2/E_1)^{0.85}$.

If we assume $G = 1/9\ E_1$, $\nu = 0.23$ Eq. (13) and Eq. (18) gives 0.26 and 0.28 for E_1/E_2=1/3 and 0.34 and 0.35 for E_1/E_2=1/3 and 2/3, respectively. This results stressed that the equation of AASH (2009) and the proposed model give quite same results.

In the cases of stiffeners consisting of star-shaped ribs, the stiffness of the ring beams was increased by the axial stiffness of the transverse stiffeners assumed to be distributed over the entire circumference, resulting in:

$$k = \frac{6\cdot E_2}{\pi}\cdot\left(\frac{t}{D}\right)^2 \quad \text{starstiffeners} \quad k = \frac{4\cdot\sin\left(30^0\right)\cdot E_2}{\pi}\cdot\left(\frac{t}{D}\right)^2 \quad \text{trianglestiffeners} \tag{17}$$

Consequently, by adding to the radial stiffness given by Eq. (16) the contribution of the transverse stiffeners and given by Eq. (17) and substituting them in Eq. (10), are derived the material strength reduction factor in the form:

$$\chi_0 = \frac{\sigma_{cr}}{\sigma_m} = \frac{0.91}{\sigma_m}\cdot\frac{t}{D}\cdot\sqrt{\frac{E_1\cdot E_2}{\left(1-\upsilon_{12}{}^2\right)}\cdot\left(\frac{E_2}{E_1}\right)^{0.85}} \quad \text{withoutstiffeners} \tag{18}$$

$$\chi = \chi_0\cdot\sqrt{1+0.47\cdot\left(1-\upsilon_{12}{}^2\right)} \quad \text{starstiffeners} \tag{19}$$

$$\chi = \chi_0\cdot\sqrt{1+0.63\cdot\left(1-\upsilon_{12}{}^2\right)} \quad \text{trianglestiffeners} \tag{20}$$

For stiffened sections the limit given by Eq. (18) can be increased by 1.20 and 1.25 for the section with star and triangular ribs (see Eqn. (19), 20).

In the case of internal and external GFRP reinforcements of PVC cross-section, if it is assumed that at failure there is no compatibility of deformation in the transverse direction between the two or three coaxial cylinders, the critical stress is the minimum between the values of the two or three cylindrical shells. Their values are given by Eq. (19–20) for the different thicknesses and materials used. In the case of a corrugated cross-section placed at a pitch s and with sides h and t (see Fig. 5) we have:

$$k = \frac{E_2\cdot h\cdot t}{\left(1-\upsilon_{12}{}^2\right)\cdot\left(D/2\right)^2}\cdot\frac{1}{s} \tag{21}$$

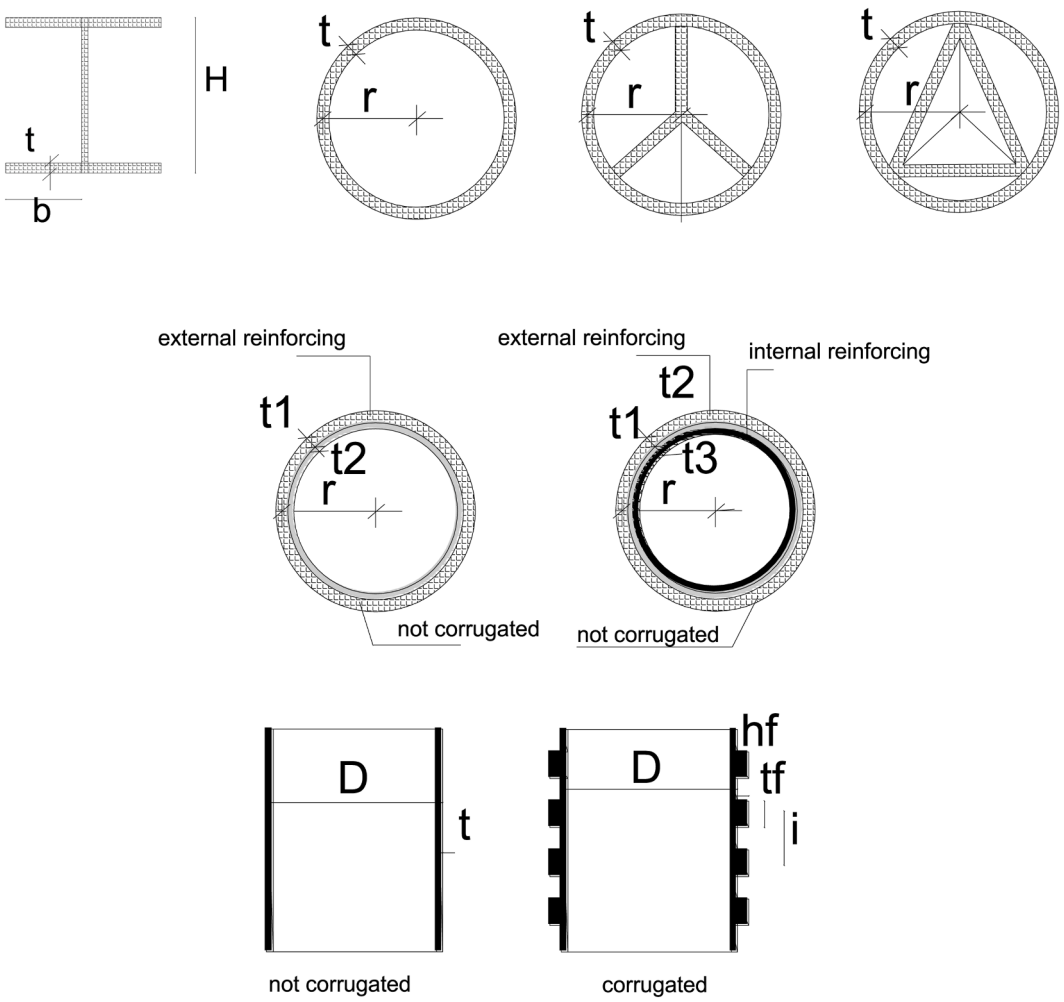

Fig. 3. double T shape and hollow circular cross-section with and withouth stiffeners.

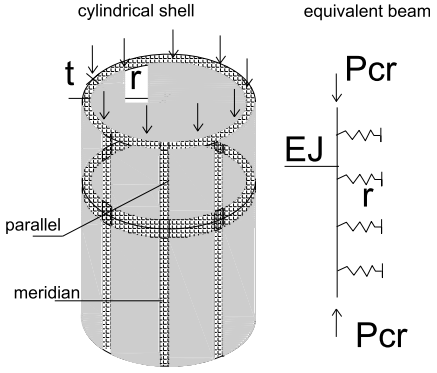

Fig. 4. Proposed model for critical stress in compression.

Fig. 5 shows the variation of the critical stress calculated with Eqn. (6,7,10) with b/t variation for double T cross-section and circular hollow cross-section.

The comparison is made for material with E_1=23 GPa, E_2/E_1=1/3, G/E_1=1/9 (with $E_1>E_2$). From the graph it can be seen that once the limit b/t = 10 is exceeded the stress is reduced due to the local instability. The same graph also shows the points relating to the experimental investigations mentioned in Cosenza and Pecce (2000) referred to double T cross-section. In the same graph there are also experimental investigation conducted by Yazhin and Babu [13], Puente et al. [14] and Yousif et al. (2024) referred to hollow cricular cross-section. It can be observed that the model of Cosenza and Pecce (2000) is the one that reproduces with the best level of approximation the trend of the experimental data available while the proposed model is the one that reproduces with a better level of approximation the trend of the experimental data available hollow circualr crosss-ection. It is evidente that second order effects are more strict in double T crosss-ection.

Fig. 6 shows the variation of the critical stress with D/t in the case of GFRP material with E_1=30 GPa, E_2/E_1=1/3, G/E_2=1/3 (with $E_1>E_2$) and in the different cases of stiffening of the cross-section.

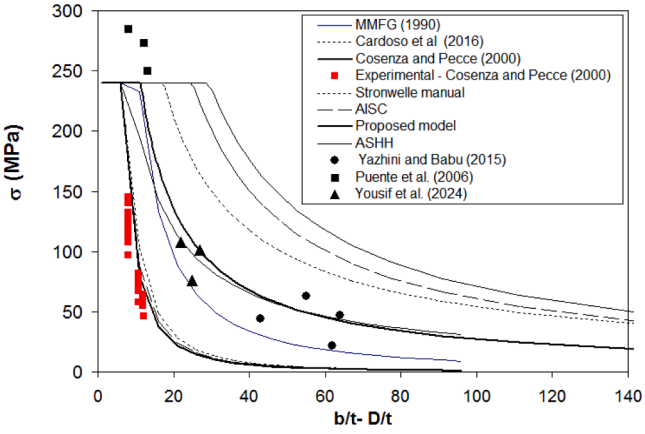

Fig. 5. Variation of critical stress with b/t and D/t for cross-section.

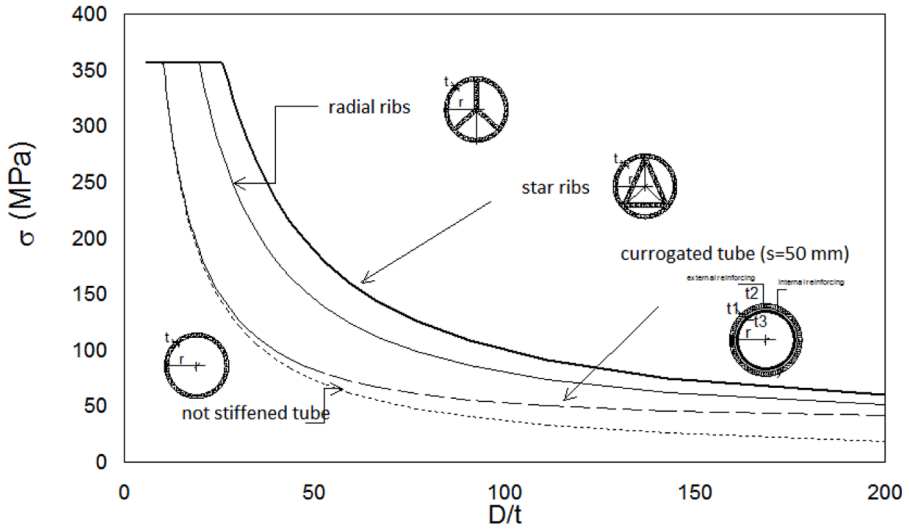

Fig. 6. Critical stress versus D/t for unstiffened and stiffened circular hollow cross-section.

From the examination of the results it is observed that the presence of stiffeners significantly increases the critical load (up to three times with respect to the cases of unstiffened cross-section) and also the limit for not having the crisis due to instability before the one due to crushing goes from 10 to 25 (from unstiffened to stiffened cross-sections). In the case of corrugated pipe the effect of the ribs is evident mainly for high values of D/t.

2.3. Ovalization of the cross-section

Another important aspect to be considered in a thin-walled hollow tubular pultruded GFRP element subjected to bending and shear is the distortion of the cross-section with shape change. As the curvature of the tube increases, the cross-section gradually changes from circular to oval as observed in Ibrahim and Polyzois (1999) and Michell and Fam [15].

Ibrahim and Polyzois (1999), based on the results of detailed finite element analyses, propose an expression for the calculation of the critical moment M_{cr} in the form:

$$M_{cr} = \frac{2\cdot\sqrt{2}}{9}\cdot\frac{\pi\cdot E_1\cdot D\cdot t^2}{\sqrt{1-\mu_{12}^2}}\cdot\left[2.1\cdot\frac{E_2}{E_1} - 0.85\cdot\left(\frac{E_2}{E_1}\right)^2\right] \tag{22}$$

Michell and Fam [15] refer to the FRP hollow tubular segment assumed to be fixed at one end and laterally loaded at the free end. At both ends, the cross-section is strengthened against ovality. The ovality is assumed to have a sinusoidal distribution along the length of the member L, with zero values at both ends. The ovality effects were assumed to be maximum at L/2 and result in a change in the moment of inertia along the length of the members with additional bending stress and increases in the deformability of the structure. The reduction of the radius in one direction is associated with an increase in the radius in the other direction and both are assumed to be equal.

A simple model (see Fig. 7) is proposed by the author, and it is presented in this section.

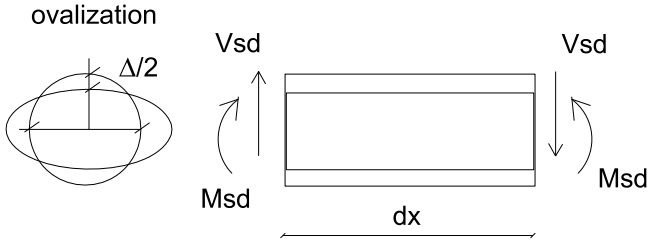

Fig. 7. Ovalization effect of cross-section under bending and shear.

The model allows one to calculate the reduction in strength and the increase in deformability of the structure due to the change in shape of the cross-section due to the lateral force F applied to the free end of a cantilever member. By adopting a model of an annular beam with diameter D, thickness t and unit depth subjected to a force $V_{sd}=F$ acting on a diametric plane (see Fig. 9), we obtain, by applying the principle of virtual work:

$$\frac{F}{2}\cdot\Delta = 2\cdot\int_0^{\pi/2}\frac{D}{12\cdot E\cdot t^3}\cdot\sin\theta\cdot d\theta \tag{23}$$

$$F\cdot L = \sigma\cdot\frac{\pi}{4}\cdot D^2\cdot t \tag{24}$$

$$\xi_O = \frac{\Delta}{D} = 1.84\cdot\left(\frac{D}{t}\right)^2\cdot\frac{D}{L}\cdot\frac{\sigma}{E} \tag{25}$$

From Eq. (25) it emerges that the ovalization is proportional to: applied stress; - square of the ratio D/t; - inversely proportional to the ratio L/D; - to the elastic modulus of the material. As the ovalization increases, the sectional moment of inertia is reduced, consequently the deformation and the stress (due to the reduction of the resistance modulus).

The critical moment is obtained by multiplying the critical stress in compression (see Eq.18) for 1.3, as suggested in Silvestre [16] and Coung [17] to take into account the bending and for strength modulus of the section obtaining the expression:

$$M_{cr} = 1.3\cdot\left[2\cdot\frac{t}{D}\cdot\sqrt{0.625\cdot\left(\frac{E_2}{E_1}\right)^{0.85}}\cdot\sqrt{\frac{E_1\cdot E_2}{3\cdot(1-\upsilon_{12}{}^2)}}\right]\cdot(0.785\cdot D^2\cdot t) \tag{26}$$

If we assume $E_2=1/3E_1$ $\upsilon_{12}=0.235$ Eqn. (24, 28) gives $M_{critical}/(E_1Dt^2)$ equal to 0.61 e 0.58, stressing that the model of Ibrahim and Polyzois (1999) (see Eq.24) and the one here proposed (Eq. (28)) gives quite same results. As shown below ASCE (2010) a reduction factor of strength of material equal to 0.65 for all cross-sections.

When ovalization effects occur J is variable with the level of force applied and varies with the expression for hollow circular cross-section:

$$J = \frac{\pi}{64}\cdot\left[D^4\cdot(1-\zeta_0)^4 - (D(1-\zeta_0) - 2\cdot t)^4\right] \tag{27}$$

the deflection of the cantilever is:

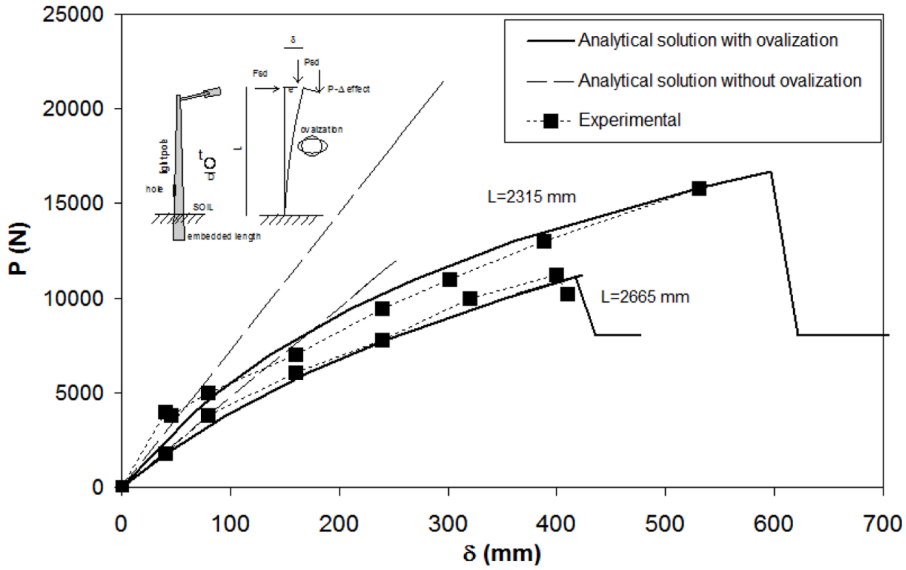

Fig. 8. Load –deflection curves (data di [15]).

$$\delta = \frac{P \cdot L^3}{3 \cdot E_1 \cdot J(\Delta)} \tag{28}$$

with P the horizontal force at the free tip of the cantilever and δ the corresponding displacement.

In this work, an average ovalization value calculated at L/2 has been assumed to take into account, t approximately, of the variation along the axis of the element of the ovalization.

Fig. 8 shows the load-deflection (P applied load at the free tip and δ the corresponding displacement) curves obtained experimentally in Micthell and Fam [15] (square symbols) and with the analytical procedure proposed here based on the use of Eqn. (27–28). Dashed lines refer to analytical preidiction of laod-deflection resposne withouth second order effects (P-Δ and ovalizatione), while continuous line refer to analytical prediction with second order effects.

The response in the absence of ovalization is also reported, highlighting the fundamental role that ovalization has on the flexural response of the element. The comparison is satisfactory for the two different lengths of elements of 2315 mm and 2665 mm tested in Micthell and Fam [15].

4. Critical load of compressed element

For GFRP compressed elements, several researchers have demonstrated, through experimental and analytical work, that the critical load of global buckling can be predicted with reasonable accuracy using the classical Euler formula [18] expressed for simple hinged elements of length L, area A and minimum inertia J as

$$P_e = \frac{\pi^2 \cdot E \cdot J}{L^2} \tag{29}$$

In Eq. (32) E is the effective modulus denoted before as E_1 which is that of pultruded in the direction of pultrusion. Its value for desing purpouses has to be reduced as suggested in CNRDT for viscosity with a reduction coefficient of 0.6 is suggested. The effective inertia considered in the calculus of critical load is the minimum inertia. The presence of ribs supposed obtaiend with same pultrusion process of hollow circular cross-sectio and with the same thickness were calcaulted on the basi of mass geometry. Details of calcualtion are not given here for brevity.

In the next sections the critical load will be presented in the graphs against the mechanical λ_c or geometrical slenderness λ expressed as:

$$\lambda_c = \sqrt{\frac{\min(\sigma_{cr}, \sigma_u) \cdot A}{P_e}} \quad \lambda = \frac{L}{(J/A)^{0.5}} \tag{30}$$

were J for hollow cross-section is:

$$J = \frac{\pi}{64} \cdot \left(D^4 - (D - 2 \cdot t)^4\right) \cong 0.39 \cdot D^3 \cdot t \tag{31}$$

For the cases of section stiffened with star and triangular ribs the inertia increases and the coefficient 0.39 of Eq. (31) has be replaced with 0.45 and 0.47, respectively for star and triangular stiffeners. The increases of the moment of inertia and therefore of the critical load were 1.15 and 1.20 time that of unstiffned element. The area of the unstiffened sections ($A = 3.14$ Dt) for the cases of section stiffened with star and triangular ribs increases of 1.47 and 1.82 times, respectively with consequent increase in the bearing capacity of 1.15×1.47=1.69 and 1.2 × 1.82=2.18.

In the case of internal and external reinforcements of PVC pipes with pultruded GFRP, if the critical stress of each cylinder is higher than the compressive strength of the material, the inertia and area are those of the full-thickness pipe (including three or two layers); while, if the critical stress of each layer is lower than the strength of the material, the critical load is that relating to the cylinder with greater slenderness and lower critical stress. Pultruded GFRP elements generally have a relatively high ratio between longitudinal elastic modulus and tangential elastic modulus. Engesser [19] highlighted that the contribution of shear in the instability load is not negligible and proposed the expression for the isotropic material:

$$P_{Eg} = P_e \cdot \frac{1}{1 + k \cdot P_e / (G \cdot A)} \tag{32}$$

The values of k suggested by Timoshenko and Gere [12] for the isotropic material are for the thin-walled circular section and for the solid tube equal to 0.5 and 0.75, respectively and 5/6 fro W shapes.

More recently, Dharmarajan (2016) proposes for the pultruded GFRP element the expression of k in the form:

$$k = \frac{6 \cdot E_{lc} \cdot (1 - m^4) \cdot (1 + m^2)}{(2 \cdot m^6 + 18 \cdot m^4 - 18 \cdot m^2 - 2) \cdot G \cdot \nu_{tl} - (7 \cdot m^6 + 27 \cdot m^4 - 27 \cdot m^2 - 7) \cdot E_{lc}} \tag{33}$$

$$\text{con } m = \frac{1}{1 - 2 \cdot t / D}$$

Comparison between buckling load calculted with Euler formula and that calculated with the proposed model, is not shown here for brevity sake,but it mainly reflects that Eulero formula do not tak intoaccount of the effects of stiffeners included in the proposed model in the variation of the effective inertia and in the modulus of elasticity calcualted, as suggested in CNRDT (2006), taking into account of the viscous effect that for a service life of 50 years reduces of 40 %.

Based on internal experimental testing, the Strongwell Corporation (2006) provided the following expression for the critical load:

$$P_e = 1.3 \cdot \frac{E_{lc} \cdot A}{(2 \cdot L/D)^{0.33}} \tag{34}$$

Puente et al. [14] proposed an equation based on the Eurocode 3 (2003) framework for steel structures in the form:

$$P_e = \frac{A \cdot F_{crl}}{0.5 \cdot \left[1 + 0.12 \cdot \left(\lambda_c{}^2 - 0.25\right) + \lambda_c{}^2\right] + \sqrt{\left\{0.5 \cdot \left[1 + 0.12 \cdot \left(\lambda_c{}^2 - 0.25\right) + \lambda_c{}^2\right]\right\}^2 - \lambda^2{}_c}} \tag{35}$$

With F_{crl} the minimum between the ultimate tensile strength of the material in compression and the critical strength of the section. Barbero and Tomblie [20] developed a design strength equation based on the results of tests on large flanged pultruded I-sections, which is currently adopted by the Italian code (CNR). The nominal compressive strength is calculated as:

$$P_e = \left[\frac{1 + 1/\lambda_c^2}{1.30} - \sqrt{\left(\frac{1 + 1/\lambda_c^2}{1.30}\right)^2 - \frac{1}{0.65 \cdot \lambda_c^2}}\right] \cdot A \cdot F_{crl} \tag{36}$$

Cardoso et al. (2006) proposed an equation to calculate the axial compressive capacity

$$P_e = \left(\frac{1 + \alpha + \lambda_c^2 \cdot \rho_p - \sqrt{\left(1 + \alpha + \lambda_c^2 \cdot \rho_p\right)^2 - 4 \cdot \lambda_c^2 \cdot \rho_p}}{2 \cdot \lambda_c^2}\right) \cdot A \cdot F_{crl} \tag{37}$$

being ρ_p the density of GFRP.

According to ASCE (2010) the maximum compressive stress is obtained with the expression:

$$\phi \cdot P_c = 0.7 \cdot A \cdot \min\left(\frac{\pi^2 \cdot E \cdot J}{L^2 \cdot A}; \sigma_{cr}; \sigma_m\right) \tag{38}$$

Fig. 9 shows the variation of the ultimate stress σ (minimum between global, local buckling and material failure) as a function of the geometric slenderness λ according to the different models considered. The theoretical values were calculated assuming E_1=30 GPa, $E_2/1/3$ E_1, $G = 1/9$ E_1 and $\nu = 0.23$. The same graph reports also the experimental data of Chen and Zhang (2024) and Zhan et al. [8] all relating to compressed elements with a hollow circular cross-section and double T cross-section given in Pecce and Cosenza [21].

From the comparison it is clear that most of the models predict with good approximation the maximum load for high values of the slenderness (between 50 and 250). If the geometric slenderness is lower than 35 the bearing capacity at least reduces of 50 % for buckling effect. Therefore, to reach this value for a wall thickness of 6 mm and a free length of 3000 mm of a simple pinned element, the external diameter of the hollow circular section must be between 175 mm. If section is stiffened, for example with the triangular system, the bearing capacity increase is 2.18 and there is no reduction in the bearing capacity for buckling effects.

Simulation of buckling behavior for the proposed new theory was not made at this stage. But Further sudies will be addressed to validate experimetnally the proposed model also utilising FEM simulation of buckling including material nonlinearities and geometric imperfections and also to confirm that the structure is stable under combined loading for the newly proposed theory .

6. Moment-axial force domain

According to the American pre-normative recommendations ASCE (2010) the domain of a structural element subjected to axial force and

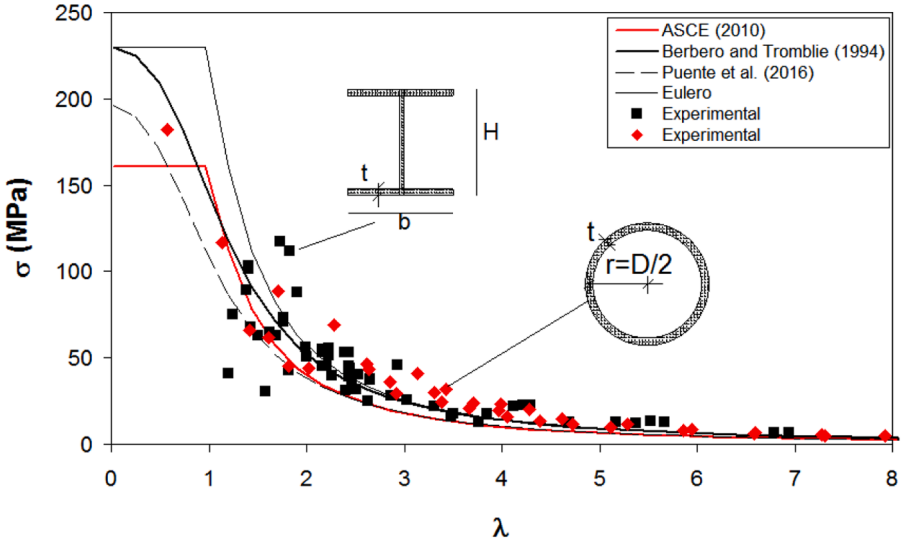

Fig. 9. Variation of critical stress for element with hollow circular and double T cross-sections.

bending moment can be assumed linear with expression:

$$\frac{P_u}{\phi \cdot P_c} + \frac{M_u}{\phi \cdot M_c} \leq 1 \tag{39}$$

where, ϕPc is the factored maximum axial compressive capacity of the member, which is the minimum of the section capacity due to crushing and the bearing capacity of the member due to global buckling; ϕMc is the factored pure bending capacity due to failure of the compressed material since the longitudinal compressive strength is greater than the longitudinal tensile strength for the FRP material.

The maximum compressive stress is given by Eq. (41) is the ultimate moment had the expression:

$$\phi \cdot M_c = 0.65 \cdot \sigma_m \cdot (2J / D) \tag{40}$$

According to the author, the moment-normal stress interaction domain can be assumed to be linear and in the form:

$$\frac{N_{sd}}{N_u} + \frac{M_{sd}}{M_u} \leq 1 \tag{41}$$

Where M_{sd}, N_{sd} are the design moment and normal stress and M_u and N_u are the ultimate moment and axial compressive force.

M_u is calculated taking into account the effect of ovalization, local buckling and material failure while, N_u is calculated as the minimum value related to global buckling, material crushing and local buckling.

$$N_u = \min\left(\sigma_{cr} \cdot A; \sigma_m \cdot A; \frac{\pi^2 \cdot E_1}{\lambda^2} \cdot \frac{1}{1 + \left(k \cdot \pi^2 \cdot E_1 / (\lambda^2 \cdot G)\right)}\right) \tag{42}$$

$$M_u = \min\left(M_m; M_{cr}\right) \tag{43}$$

with

$$M_{cr} = 0.93 \cdot 9 \cdot D \cdot t^2 \cdot \sqrt{\frac{E_1 \cdot E_2}{1 - v_{12}^2}} \left(\frac{E_2}{E_1}\right)^{0.85} \tag{44}$$

$$M_m = 0.78 \cdot D^2 \cdot t \cdot \frac{E_1}{100} \tag{45}$$

The model considers reduction of critical stress due to buckling effects only referring to uniform stresses induced by compression. In the case of flexure or axial force and bending moment the critical stress was that dedcued with the proposed model increased of 1.3 as suggested in the literature [16]. Further studies will be addressed to analyze more in details these cases.

If we impose that $M_{cr} < M_u$ it resutls:

$$\frac{M_{cr}}{M_m} = 119 \cdot \frac{t}{D} \cdot \sqrt{\frac{1}{(1 - v_{12}{}^2)}} \cdot \left(\frac{E_2}{E_1}\right)^{1.85} \leq 1 \tag{46}$$

and therefore for v_{12}=0.23 and E_2/E_1 equal to 1/3 and 2/3 we obtain $D/t < 44$ and 80, respectively.

Fig. 10 shows the strength domain derived with the ASCE (2010) procedure and with the proposed model.

The same graph shows the domain obtained by the author taking into account only the material strength. In addition graph gives the experimental points of the investigation recently conducted by Higgoda et al. (2023). The experimental data refer to tubular profiles with hollow circular cross-section of diameter 114 mm and thickness 6.4 mm with different L/D values equal to 9, 12 and 15. The eccentricities considered are 0, 28.5 and 57 mm. The material has an elastic modulus of 33,250 MPa and a compressive strength of 268 MPa. The comparison shows that the ASCE (2010) model captures the strength reductions of the gross-domain only referred to strength of material for the effects of local, global and ovalization buckling, but the proposed model interprets better the trend of the experimental data.

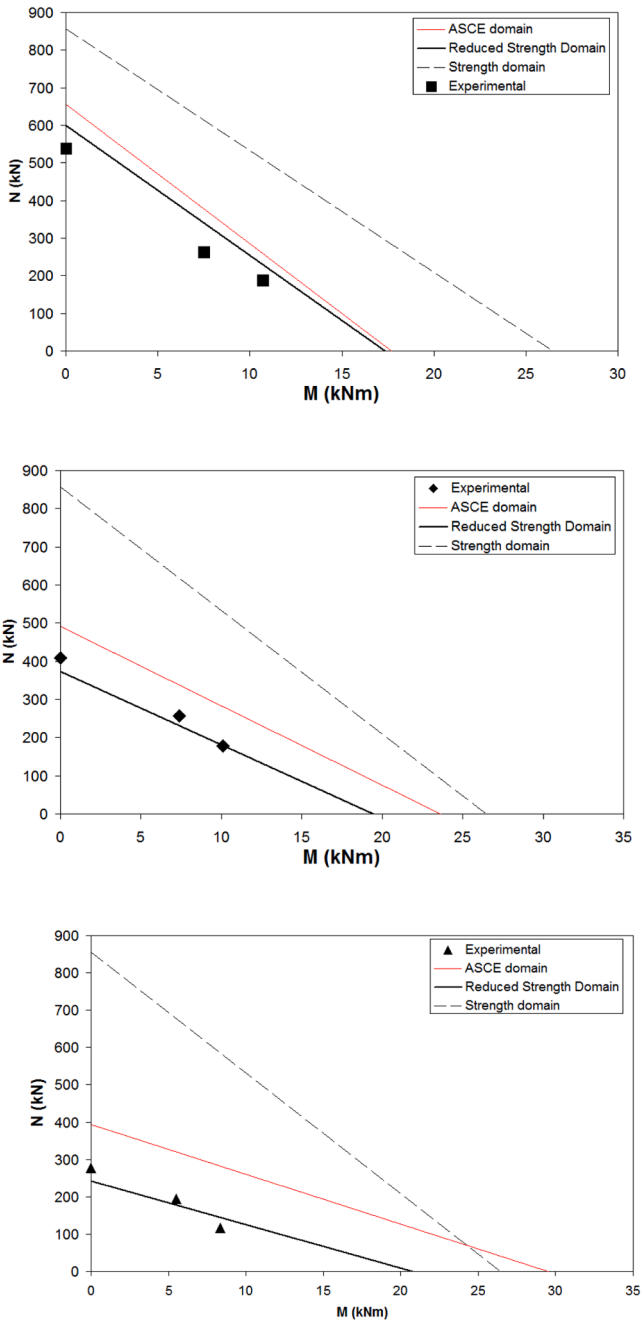

Fig. 10. Strength domain for L/ D : a) 9, b) 12, c) 15. Data of Higgoda et al. (2023).

7. Conclusions

In this work, the expressions of the local and global critical buckling load for hollow circular GFRP profiles pultruded with different types of internal stiffeners are reported. The proposed model allows to obtain a simple expression of the critical buckling load of a hollow circular section pultruded tube with internal stiffeners treated as a compressed cylinder of small thickness and idealized as a set of meridians and parallels of GFRP fiber beams connected to each other and interacting with a containment action of the parallels on the meridians. The results obtained with the proposed model allow to make the following conclusive considerations:

- in compression the limit diameter/thickness ratio that avoids the buckling crisis before crushing is equal to 10 for a profile without stiffeners and between 18 and 25 for a profile with stiffeners;
- the increase in strength for global instability due to the presence of reinforcements in the section produces increases of the order of 20 % compared to the case of elements with an unstiffened section;
- the ovalization of the section in bending or compressive bending significantly penalizes the bending capacity of the section (40 %) and increases its deflection (100 %); • most of the models considered, including the Euler model, predict with good approximation the maximum load for high values of the slenderness (between 50 and 250);
- in bending the limit diameter/thickness ratio that avoids the buckling crisis before crushing is in dependence of the ratio of elastic module (1/3 and 2/3) between 40 and 80 for a profile without stiffeners;
- in the case of member with not stiffened cross-section and with geometric slenderness close to 50 the load bearing capacity reduced of 50 %, but with stiffened cross-section the whole bearing capacity is reached.

CRediT authorship contribution statement

Giuseppe Campione: Writing – original draft, Formal analysis.

Declaration of competing interest

The authors declare that they have no known competing financial interests or personal relationships that could have appeared to influence the work reported in this paper.

Data availability

No data, models, or code were generated or used during the study.

References

[1] M. Alhawamdeh, O. Alajarmeh, T. Aravinthan, T. Shelley, P. Schubel, M. Kemp, X. Zeng, Modelling hollow pultruded FRP profiles under axial compression: local bukling and progressive failure, Compos. Struct. 262 (2021) 113650.
[2] L. Gadner, A. Fieber, L. Marcorini, Formulae for calculating elastic local buckling of full structural cross-sections, Structures 17 (2019) 2–20.
[3] A. Godat, F. Légeron, V. Gagné, B. Marmion, Use of FRP pultruded members for electricity transmission towers, Compos. Struct. 105 (2013) 408–421, 2013.
[4] S. Metiche, R. Masmoudi, Full-scale flexural testing on Fiber-reinforced polymer (FRP) poles, Open Civil Eng. J. 107 (37) (2007) 37–50, https://doi.org/10.2174/1874149500701010037, 107(37):37-50.
[5] F. Nunes, N. Silvestre, J.R. Correia, Structural behavior of hybrid FRP pultruded columns. Part 2: numerical study, Compos. Struct. 139 (2016) 304–319.
[6] Z. Sun, J. Zhong, Y. Zhan, J. Hao, Q. Zhao, Experimental study on the axial compression performance of pultruded GFRP tubes for emergency bridges, Structures 63 (2024) 106466.
[7] M. Kasiviswanathan, M. Anbarasu, Numerical study and design rule for axial capacities of pultrude GFRP hollow columns, Structures 39 (2022) 253–265.
[8] Y. Zhan, G. Wu, K.A. Harries, Determination of critical load for global flexural buckling in concentrically loaded pultruded FRP structural struts, Eng. Struct. 158 (2018) 1–12.
[9] C. Zhang, Y. Chen, M. Dou, Axial compression behavior and modeling of pultrude basal-fibre-reinforced polymer (BFRP) tubes, Buildings 13 (2023) 1397.
[10] H. Zhang, F. Li, A review of prediction methods for global buckling critical loads of pultruded FRP struts, Compos. Struct. 329 (2024) 1177752.
[11] D.C.T. Cardoso, K.A. Harries, E. Batista, M. de, Compressive strength equation for GFRP square tube columns, Compos. Part B 59 (2014) 1–11, https://doi.org/10.1016/j.compositesb.2013.10.057.
[12] S.P. Timoshenko, J.M. Gere, Theory of elastic stability, McGraw-Hill, New York, 1961.
[13] A. Yazhini, B.C. Ramesh, Behavior of circular glass fiber reinforced polymer tubes under axial compression, Int. J. Sci. Eng. Applic. 4 (3) (2015) 110–116.
[14] I. Puente, A. Insausti, m. Azkune, Buckling of GFRP columns: an empirical approach to design, J. Compos. Construct. ASCE 10 (6) (2006) 529–537.
[15] J. Mitchell, A. Fam, Tests and analysis of cantilevered GFRP tubular poles with partial concrete filling, J. Compos. Construct. 14 (1) (2010). February 1, 2010.
[16] N. Silvestre, Generalized beam theory to analyze the buckling behavior of circular cylindrical shell and tubes, Thin-walled Struct. 45 (2007) 185–198.
[17] B.H. Coung, Local buckling of thin-walled circular hollow section under uniform bending, J. Sci. Technol. HUCE (NUCE) 15 (4) (2021) 88–98.
[18] Eulero L. De Curvis Elasticis. 20(58), Bruges, Belgium; 1933. (Methodus inveniendi lineas curvas maximi minimive proprietate gau dentes, 1744, Lausanne).
[19] F. Engesser, Die Knickfestigkeit gerader Sfäbe, Centralblatt der Bauverwaltung 11 (1891) 483 [111]Haringx JA. On.
[20] E. Barbero, J. Tomblin, A phenomenological design equation for FRP columns with interaction between local and global buckling, Thin-Walled Struct 18 (2) (1994) 117–131, 1994.
[21] M. Pecce, E. Cosenza, Local buckling curves for the design of FRP profiles, Thin-walld Struct. 37 (2000) 207–222.